

Acute pulmonary and moderate cardiovascular responses of spontaneously hypertensive rats after exposure to single-wall carbon nanotubes

Cuicui Ge, Li Meng, Ligeng Xu, Ru Bai, Jiangfeng Du, Lili Zhang, Yang Li, Yanzhong Chang, Yuliang Zhao & Chunying Chen

To cite this article: Cuicui Ge, Li Meng, Ligeng Xu, Ru Bai, Jiangfeng Du, Lili Zhang, Yang Li, Yanzhong Chang, Yuliang Zhao & Chunying Chen (2012) Acute pulmonary and moderate cardiovascular responses of spontaneously hypertensive rats after exposure to single-wall carbon nanotubes, *Nanotoxicology*, 6:5, 526-542, DOI: [10.3109/17435390.2011.587905](https://doi.org/10.3109/17435390.2011.587905)

To link to this article: <https://doi.org/10.3109/17435390.2011.587905>




View supplementary material 



Published online: 09 Jun 2011.



Submit your article to this journal 



Article views: 166



Citing articles: 39 View citing articles 

Acute pulmonary and moderate cardiovascular responses of spontaneously hypertensive rats after exposure to single-wall carbon nanotubes

CUICUI GE^{1*}, LI MENG^{1*}, LIGENG XU¹, RU BAI¹, JIANGFENG DU², LILI ZHANG¹, YANG LI³, YANZHONG CHANG³, YULIANG ZHAO¹, & CHUNYING CHEN¹

¹CAS Key Lab for Biomedical Effects of Nanomaterials and Nanosafety, Institute of High Energy Physics and National Center for Nanoscience & Technology of China, Chinese Academy of Sciences, Beijing, ²School of Chemistry and Chemical Engineering, University of South China, Hengyang, and ³Laboratory of Molecular Iron Metabolism, College of Life Science, Hebei Normal University, Shijiazhuang, P. R. China

(Received 20 December 2010; accepted 27 April 2011)

Abstract

As a novel kind of nanomaterial with wide potential applications, the adverse effects of carbon nanotubes (CNTs) have recently received significant attention after respiratory exposure. In this study, single-wall carbon nanotubes (SWCNTs) containing different metal contents were intratracheally instilled into lungs of spontaneously hypertensive rats. Pulmonary and cardiovascular system alterations were evaluated at 24 and 72 h post-instillation. Biomarkers of inflammation, oxidative stress and cell damage in the bronchoalveolar lavage fluid (BALF) were increased significantly 24 h post-exposure of SWCNTs. The increased endothelin-1 levels in BALF and plasma and angiotensin I-converting enzyme in plasma suggested endothelial dysfunction in the pulmonary circulation and peripheral vascular thrombosis. These findings suggest that respiratory exposure to SWCNTs can induce acute pulmonary and cardiovascular responses and individuals with existing cardiovascular diseases are very susceptible to SWCNTs exposure. The co-existence of metal residues in SWCNTs can aggravate the adverse effects.

Keywords: Intratracheal instillation, single-wall carbon nanotube, metal residues, cardiovascular effect, pulmonary toxicity

Introduction

Several epidemiological and clinical studies have provided evidence that inhalation of ultrafine particles (UFP, diameter <100 nm) contributes to pulmonary and cardiovascular systemic morbidity and mortality in susceptible populations (Liu et al. 2003; Elder et al. 2007; Rückerl et al. 2007; Delfino et al. 2008) and increases the risk of respiratory and cardiovascular diseases of human (Samet et al. 2000; Donaldson et al. 2001; Gauderman et al. 2004). As a fibre-shaped nanoparticle, single-wall carbon nanotubes (SWCNTs) with unique electronic and mechanical properties have a diameter ranging from 0.7–1.5 nm with lengths >1 µm. The versatile chemistry of carbon nanotubes (CNTs) enables a wide range of their applications in biomedicine, such as *in vivo* cancer

therapy, drug delivery, gene therapy, photothermal therapy and radiofrequency (RF) ablation therapy. Along with the potential widespread applications, the potential for occupational exposures to carbon nanotubes is increasing.

Previous toxicological studies demonstrated that SWCNTs exposure caused accumulation of carbon nanotube aggregates in the lung, followed by the rapid formation of pulmonary granulomatous at the site (Lam et al. 2004; Warheit et al. 2004; Muller et al. 2005; Shvedova et al. 2005; Poland et al. 2008). The lung is believed to be the prime target for SWCNT toxicity through inhalation exposure especially in occupational settings. Biological and toxicological responses to CNTs may vary by dose, route of dosing, and type of CNTs. Reported researches on the pulmonary *in vivo* toxicity of CNTs to date have been

Correspondence: Dr Chunying Chen, National Center for Nanoscience & Technology of China, No. 11, Beiyitiao, Zhongguancun, Beijing 100190, P. R. China. Tel: +86 10 82545520. Fax: +86 10 62656765. E-mail: chenchy@nanoctr.cn

*C. Ge and L. Meng contributed equally to this paper

conducted by either instillation into the trachea (Lam et al. 2004; Warheit et al. 2004; Muller et al. 2005; Chou et al. 2008) or pharyngeal aspiration (Shvedova et al. 2005, Muller et al. 2008; Ma-Hock et al. 2009; Ryman-Rasmussen et al. 2009). Each of these publications reported significant pulmonary effects, including inflammation, evidence of oxidative stress, fibrosis (Shvedova et al. 2008) and granuloma formation (Lam et al. 2004; Warheit et al. 2004; Muller et al. 2005; Shvedova et al. 2005). The pulmonary inflammatory, oxidative stress are dose and time-dependent (Porter et al. 2010; Kobayashi et al. 2010).

Some experiments have further evaluated the association between pulmonary and systemic immune responses after respiratory exposure (Mitchell et al. 2007). Lung instillation of SWCNTs induced a dose-dependent increase in oxidative vascular damage and affected atherosclerosis progression in ApoE^{-/-} transgenic mice (Li et al. 2007). In addition, after carbon nanotube depositing in the lung, acute local and systemic responses were activated that were characterized by the combination of blood gene expression and circulating soluble protein analysis. These results demonstrated a close cross-talk between lung and systemic circulation after carbon nanotube respiratory exposure. The systemic response, if it is chronic and persistent, may trigger or exacerbate cardiovascular dysfunction and disease, such as atherosclerosis (Erdely et al. 2008).

Metal particle catalysts are essential in the mass production of nanotubes by chemical vapor deposition (CVD). Removal of these residual catalysts (typically Fe, Co, Mo, Ni and/or Y) after CNTs production is one of the key challenges for the application of CNTs in many fields. It is of great concern that the results of toxicological and ecological impact studies of carbon nanotubes could be misinterpreted due to the presence of impurities in the test materials. The previous studies also indicate that metal residues in CNTs can mobilize from solid phase into metal ion and these mobilized metals can cause cytotoxicity to some degree (Guo et al. 2007; Liu et al. 2007, 2008). The toxicity of CNTs has a close relationship with metal impurities which can generate reactive oxygen species (ROS) via the Fenton reaction (Smart et al. 2006; Pulskamp et al. 2007; Murray et al. 2009).

Hypertension is already a highly prevalent cardiovascular risk factor worldwide because of increasing longevity and prevalence of contributing factors such as obesity. WHO estimated that hypertension causes 4.5% of the current global disease burden and is as prevalent in many developing and developed countries. Blood pressure-induced cardiovascular risk rises continuously. Currently, there are more than 200 million hypertensive patients in China. The literature

data show that particle exposure may trigger acute cardiac events as well as promote the chronic development of cardiovascular disorders. Spontaneously hypertensive rats are a model of human essential hypertension widely used in testing antihypertensive drugs and analyzing the reaction of these animals to a wide range of stimuli. Some researches have used the animal model to evaluate the role of these host susceptible factors associated with mortality and morbidity when exposed to particulate matter (Bagate et al. 2004; Cao et al. 2007).

There are no previous reports to assess the potential cardiovascular impact after exposure to SWCNTs containing different metal residues as far as we know. The whole blood cell expression closely represented the CNT-induced lung and systemic toxicity related to possible cardiovascular outcomes (Erdely et al. 2008). Therefore, the direct evidence and the underlying pathophysiological mechanisms linking SWCNTs and cardiovascular morbidity need to be elucidated. Spontaneously hypertensive (SH) rat is considered a good animal model of human essential or primary hypertension, and has been extensively used to study cardiovascular disease. Like in human beings, the hypertensive response starts with advancing age in this strain of rats and the cause of the rising blood pressure remains unknown. Rise in blood pressure begins around 5–6 weeks of age and the systolic pressures may reach values between 180 and 200 mmHg in the adult. Starting between 40 and 50 weeks, SH rat develops characteristics of cardiovascular disease, like hypertrophy of heart and blood vessels. Some of these may develop still higher blood pressure and die of stroke. Therefore SH rat would be more susceptible to fine particles when compared to normal rats (Vanhoutte 1997; Badr and Wainwright 2004; Cao et al. 2007). In our present study, we compared the pulmonary and cardiovascular effects of SWCNTs with different residue metal impurities that enable us to understand the contribution both of carbon nanotubes and metal impurities in hypertension sensitive rats.

Materials and methods

Materials and characterization

Two kinds of single-wall carbon nanotubes were provided by Shenzhen Nanotechnologies Co., Ltd (NTP), named as Fe-poor and Fe-rich SWCNTs based on their metal impurities. High-resolution transmission electron microscopy (HRTEM, Tecnai G2 F20 U-TWIN) was used to characterize the morphology of SWCNTs and inductively coupled plasma-mass spectrometry (ICP-MS, Thermo

Elemental X7, Thermo Electron Co.) was employed to provide a quantitative analysis of the metal residues. The suspension of 1.5 mg/mL SWCNT was prepared by dispersing SWCNT powders in saline solution containing 0.5% F108 and sonicated for 30 min before using. The chemical composition of artificial fluid is listed (Supplementary Table S1, available online). The mobilization of metal residues from SWCNTs into artificial fluid was investigated and the experimental detail is available in the online Supplementary material.

Reagent for ICP-MS determination

All the reagents were analytical purity and higher. Ultrapure water (18 M Ω) was obtained from a Milli-Q water-purification system (Millipore, UK). The QC-21 quality control standard solution and indium standard solution were obtained from SPEX Plasma Standard, SPEX, Menlo Park, NJ, USA. Stock standard solutions were obtained as 1000 mg/L⁻¹ of each metal (As, Be, Ca, Cd, Co, Cr, Cu, Fe, Li, Mg, Mn, Mo, Ni, Pb, Sb, Se, Sr, Ti, Tl, V, Zn) (GBW 08617, National Research Centre for CRMs, China). The working standards were diluted as required daily.

Mobilization of metal residues from CNTs into artificial fluids and ICP-MS measurements

Two artificial biological fluids were prepared by dissolving appropriate quantities of the precursor chemicals in deionized water, with inorganic constituents nearly equal to those of Supplementary Table S1 (available online). SWCNT suspensions (1.5 mg/mL) were prepared by dispersing SWCNT powder in two artificial biological fluids. The obtained suspensions were incubated in 37°C at 100 r/min. Following settlement, 1 mL of each supernatant was taken out and the same volume of biological fluid was supplied into the suspension. The 1 mL of each supernatant was transferred to a centrifugal tube that was centrifuged at 10000 rpm for 15 min twice to remove any free particles. In this way, clear leachates could be obtained free of suspended powders. The obtained leachates were two-fold diluted using 4% HNO₃. Finally, the elements in the obtained clear diluted solution were analyzed by a Thermo Elemental X7 ICP-MS.

Animal exposure and sacrifice

Male spontaneously hypertensive (SH) rats (derived from WKY rats by segregation of the hypertensive trait and inbreeding), 11–12 weeks old and 220–250 g

body weight, were obtained from Vital River Laboratory Animal Technology Co., Ltd. Animals were housed in macrolon cages Type 3 in a room with HEPA-filtered air and a constant climate (room temperature 21 \pm 2°C and relative humidity 40–70%) with a 12-h light/dark cycle (light on at 08:00 h). Rodent food and tap water via an automatic drinking-water system was supplied *ad libitum*. Experiments were approved according to the Ethics Committee of Animal Care and Experimentation of the National Institute for Environmental Studies, China. All rats used were treated humanely. SH rats were randomized by body weight into groups of control, saline, Fe-poor SWCNTs and Fe-rich SWCNTs (6 rats/group). The doses of 40–500 μ g per mice and 50 μ g–5 mg per rat were usually used for evaluation of pulmonary toxicity by intratracheal instillation in previous studies. In our present study, the SH rats were exposed to two kinds of saline-suspended SWCNT particles (0.6 mg/rat) using a non-surgical intratracheal instillation and the exposure was administered once a day for two continuous days. Then, the rats were killed after 24 and 72 h following the last exposure. At necropsy, animals were anesthetized with 40 mg/kg intraperitoneal sodium pentobarbital and sacrificed by exsanguination via the abdominal aorta.

Preparation and biochemical analysis of bronchoalveolar lavage fluid

The right lung was used to obtain BALF after ligation of the left bronchus. The right lung was lavaged three times with a volume of phosphate-buffered saline (PBS, pH 7.4) according to 27 mL/kg body weight at 37°C. The recovered BALF was placed on ice. One aliquot of the recovered lavage fluid was centrifuged (400 g, 10 min, 4°C) and the pellets were collected for cell counts and differentiation.

For differential cell counts of polymorphonuclear neutrophilic leukocyte (PMN), macrophages and lymphocytes, cytospin slides were made and stained with Giemsa and 200 cells were counted. The supernatant fluid was immediately collected in different tubes, frozen at –80°C and avoided repeated freeze/thaw. The BAL fluid was used to evaluation of cellular toxicity (lactate dehydrogenase [LDH, EC 1.1.2.3] activity, albumin [ALB], total protein [TP], Clara cell 16 protein [CC16], heme oxygenase-1 [HO-1, EC 1.14.99.3]), inflammation (tumor necrosis factor [TNF- α], interleukin-6 [IL-6], macrophage inflammatory protein-2 [MIP-2], neutrophil activity marker myeloperoxidase [MPO, EC 1.4.3.6]), and endothelin-1 (ET-1).

The activity of LDH and content of ALB, TP in BAL fluids were assayed using kits provided from

Nanjing Jiancheng Bioengineering Institute, China. The other Elisa kits were provided from USCN Life Science Inc., Wuhan, China.

Blood analysis

Serum or plasma samples were collected following the standard operation procedures for routine blood draw. About 8 mL of whole blood was collected from the abdominal aorta, 2 mL were directly put into blood collection tubes containing EDTA (for hematological analysis), then 3 mL into collection tubes containing citrate as anticoagulants (for plasma protein analysis), and finally another 3 mL whole blood were transferred into normal collection tubes (for serum analysis). The harvest serum and plasma were frozen at -80°C and avoided repeated freeze/thaw. Biomarkers of inflammation (C-reactive protein [CRP] and TNF- α), inter cellular adhesion molecule (ICAM)-1, endothelin-1 (ET-1) and vascular responses (fibrinogen and von Willebrand factor [vWF], angiotensin I-converting enzyme [ACE, EC 3.4.15.1]) were analyzed subsequently. The fibrinogen, ET-1, ACE, and vWF in citrate plasma and ICAM-1, TNF- α and CRP contents in serum were measured using commercial enzyme-linked immunosorbent assay (ELISA) kits provided by Usen Life Science Inc., Wuhan, China. The absorbance was measured using a microplate reader (Tecan Infinite M200, Japan).

Histopathological examination

The left lung and left ventricle of each group were dissected and immediately fixed with 10% phosphate buffered formalin for stained with Harris' hematoxylin and eosin (H&E). After HE staining, the sections were photographed using an optical microscope (Leica DM4000M, Germany). The identity and analysis of the pathology sections were blind to the pathologist.

Ultrastructure of lung tissue by transmission electron microscopy

The fresh tissue samples were immersed in 2.5% glutaraldehyde at 4°C . After washing with phosphate buffer solution sufficiently, they were fixed with 1% osmium tetroxide, dehydrated in a graded series of ethanol, and embedded in araldite, polymerized for 24 h at 37°C . Ultrathin sections (50 nm) were cut with an ultramicrotome (LKB-V, Sweden), contrasted with uranyl acetate and lead citrate, and finally observed with TEM (H-600, Hitachi) by an independent pathologist.

Statistical analysis

Values were expressed as mean \pm standard deviation (SD). Statistical evaluation was conducted using Statistical Packages for the Social Sciences (SPSS Inc., Chicago, USA). Data were analyzed and significance of the differences between control and exposure groups and differences within exposure time was determined by one-way ANOVA with Dunnett's post hoc tests. Results were considered significant at $*p < 0.05$ and $**p < 0.01$.

Results

Characteristics and morphology of SWCNTs

The existence of metal residuals contained in two kinds of SWCNTs is clearly shown in their HRTEM images (Figures 1A, 1B). ICP-MS analysis provided direct quantitative results of the metal impurities (Table I). The total metal mass percentages were respectively 5.4% and 6.5%. The significant quantity of Fe, Co, and Mo implied these metals were employed as the catalyst metals in the synthesis of SWCNTs. SWCNT containing 1.07% Fe was named as Fe-rich SWCNTs and SWCNT containing 0.11% Fe was named as Fe-poor SWCNT.

The leaching of metal residues from SWCNT into artificial fluids

Due to encapsulation in carbon shell, these catalyst residues might be partially bio-available. Therefore, the dissolution rates were investigated via monitoring the biological microenvironment.

As shown in Figure 1C and 1D, the concentrations of Fe leached from 1.5 mg SWCNTs into 1 mL artificial lysosomal fluid can reach 282 and 411 ppb for Fe-poor SWCNT, 3185 ppb and 5371 ppb for Fe-rich SWCNT from 1–3 d of incubation, respectively. There were similar tendency in Gamble's solution and mainly Co and Mo could be leached from CNTs. The other metals are not detectable from the leached fluids. The mobilization rates of metal residues from SWCNTs into artificial fluids were calculated (Table II). After incubation of 1 and 3 d, the mobilization rates of Fe in the weakly acidic ALF (pH = 4.5) were from 16.5–33.4%, Co from 0.9–1.3%, and Mo from 5.8–13.1%. In the neutral Gamble's solution, the mobilization rates of Co were from 0.5–0.6% and Mo from 5.5–8.4%.

Bronchoalveolar lavage fluid (BALF) analysis

Inflammation. The pulmonary exposure to SWCNTs by non-surgical intratracheal instillation resulted in

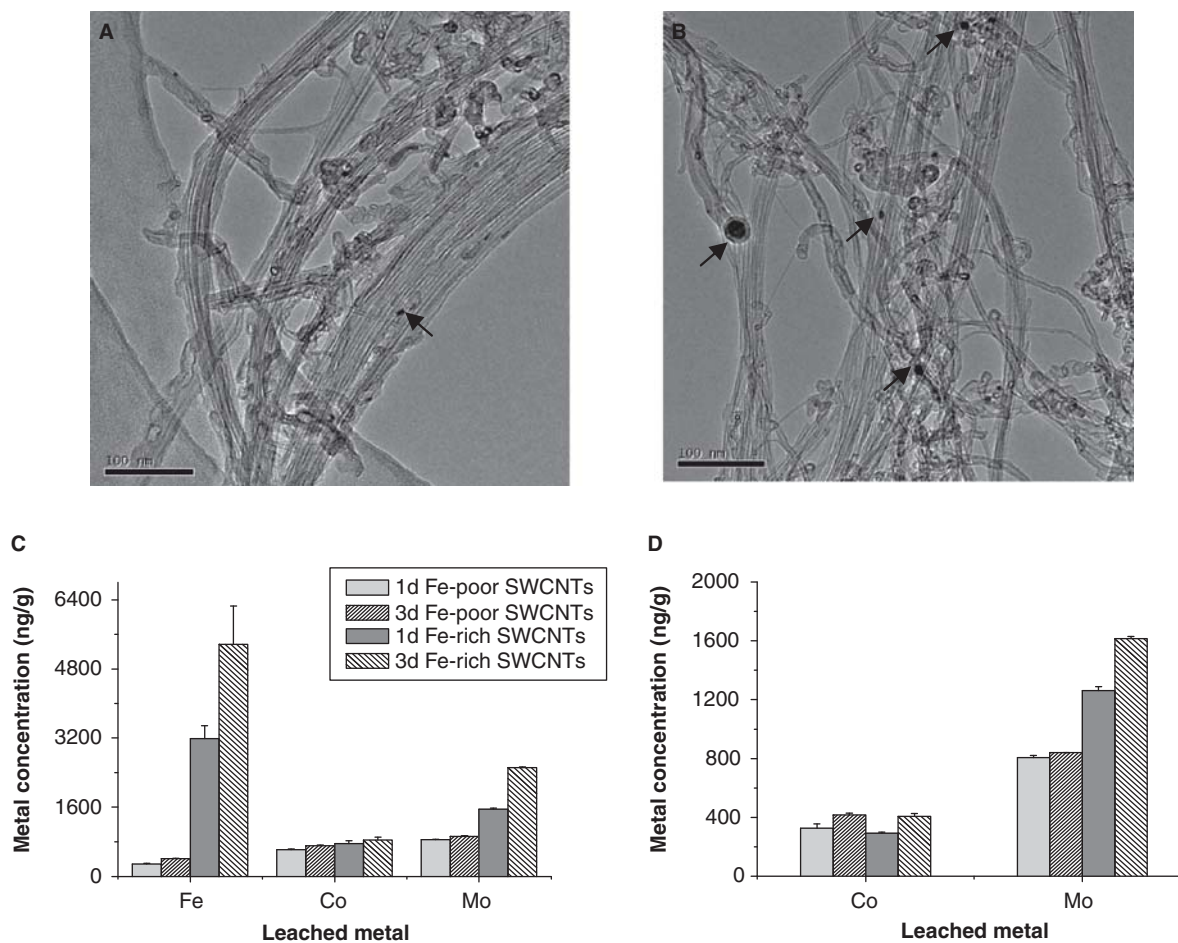


Figure 1. HRTEM image and ICP-MS analysis of leached metal of SWCNTs. (A) HRTEM image of Fe-poor SWCNTs. (B) HRTEM image of Fe-rich SWCNTs, black arrows point to metal residues. (C, D) The concentration level of metal leached from 1.5 mg SWCNTs into 1 g artificial lysosomal fluid (pH = 4.5) and Gamble's solution (pH = 7.4), respectively. Unit: ng/g.

Table I. The contents of metal impurities in the SWCNTs determined by ICP-MS. Data are expressed as mean \pm standard deviation of three independent determinations ($\mu\text{g/g}$).

	Co	Cr	Cu	Fe	Mo	Ni	Total metal
Fe-poor SWCNTs	43200 \pm 141	537 \pm 53	15 \pm 2	1142 \pm 87	9712 \pm 10	58 \pm 1	54664 \pm 294
Fe-rich SWCNTs	41700 \pm 1414	10 \pm 1	7 \pm 0.4	10700 \pm 282	12850 \pm 1767	18 \pm 1	65285 \pm 3465

increases of several inflammatory markers in the BALF. BALF cell differentials were performed to evaluate inflammatory response after SWCNTs exposure. Total cell numbers were increased with SWCNTs treatment. Compared with saline group, the number of PMNs was significantly elevated after exposure to Fe-poor SWCNTs ($p < 0.05$) and Fe-rich SWCNTs ($p < 0.01$) (Figure 2A). The significantly elevated number of lymphocytes was only found in the Fe-rich SWCNTs group (Figure 2B). The number of macrophages was significantly higher after exposure to both SWCNTs at 3 d post-exposure ($p < 0.05$, Figure 2C). The percentages

of PMNs, and lymphocytes were increased by counting 200 cells (Supplementary Table SII, available online). Myeloperoxidase (MPO) is a plentiful constituent of neutrophils and its activity therefore is a direct measure of PMN amount and an indirect indicator of lung injury. Consistent with the number of PMN, MPO activity was significantly increased at 24 h post-exposure ($p < 0.01$) and decreased partly at 72 h post-exposure but it was still significantly higher than saline groups ($p < 0.05$, Figure 2D). The neutrophil cells and SWCNTs (arrow)-laden macrophage cells in BALF are shown in Figure 2E and 2F.

Table II. The weight percentage of each released metal accounting for total metal content in SWCNTs at each indicated time point (wt.%).

Artificial fluid	SWCNTs	Incubation time	Fe	Co	Mo
Lysosomal fluid (pH = 4.5)	Fe-poor	1 d	16.5 ± 1.5	0.9 ± 0.02	5.8 ± 0.06
		3 d	24 ± 0.5	1.1 ± 0.03	6.3 ± 0.1
	Fe-rich	1 d	19.8 ± 1.8	1.2 ± 0.1	8.1 ± 0.1
		3 d	33.4 ± 5.5	1.3 ± 0.1	13.1 ± 0.1
Gamble's solution (pH = 7.4)	Fe-poor	1 d	ND	0.5 ± 0.04	5.5 ± 0.1
		3 d	ND	0.6 ± 0.02	5.7 ± 0.05
	Fe-rich	1 d	ND	0.5 ± 0.01	6.5 ± 0.1
		3 d	ND	0.6 ± 0.03	8.4 ± 0.07

ND, not detectable.

In addition to post-exposure time, the role of metal impurity in CNT was also considered. At the same time point, exposure to Fe-rich CNT caused a significant increase of PMN and lymphocyte than exposure to Fe-poor CNT ($p < 0.01$, Figure 2A and 2B). The MPO activity in Fe-rich CNT group was higher than in Fe-poor CNT group at the same time point, which is in agreement with the numbers of PMN (Figure 2A, 2D). Many studies attribute the toxicity of CNTs to the metal residues which can generate ROS. In this study, the Fe content in both SWCNTs were not high, one is 1% and the other is 0.1% (wt.%). The mobilized rates of Fe nanoparticles were large, and the Fe content mobilized from Fe-rich SWCNT was more than 10 times that of Fe-poor SWCNTs. However, due to the low Fe content, the effect of different Fe content on inflammatory was not very evidently different.

Toxicity. The pulmonary exposure to CNT caused the augmented cytotoxicity and damaged cell integrity by measuring LDH, albumin, and total protein in the BALF (Figure 3). The leakage of LDH is a biomarker of dead or membrane damaged cells. LDH activity was significantly increased in BALF at 24 h and there was a tendency of lasting increase at 3 days post-exposure ($p < 0.01$, Figure 3A). Total protein and albumin mainly come from the plasma exudation. The alveolar membrane and pulmonary capillary membrane of normal structure and function can prevent the passing of albumin. Alveolar epithelial barrier injury is frequently associated with increased contents of ALB and TP in BALF. The concentrations of total protein and albumin in BALF were significantly elevated at 24 and 72 h post-exposure ($p < 0.05$), respectively, which indicated the vascular permeability and cellular damage within the lung tissues (Figure 3B and 3C). The levels of albumin in two exposure groups had a small decrease at 72 h post-exposure if compared with those at 24 h.

The significant increases of LDH, total protein and albumin demonstrate that SWCNT exposure can bring an acute pulmonary damage and the injury had not recovered within 72 h. In addition, the levels of LDH, total protein, and albumin of Fe-rich CNT group were higher than Fe-poor CNT group, which indicated a more pronounced response induced by excessive metal impurities in SWCNTs.

Cytokine and oxidative stress. The exposure to SWCNTs by instillation amplified the concentrations of pro-inflammatory cytokines in BALF. The TNF- α concentration was significantly elevated at 24 h post-exposure and almost seven times higher than saline groups ($p < 0.01$, Figure 3D). This effect was significantly decreased at 72 h post-exposure (vs. 24 h post-exposure, $p < 0.05$) and was still four times higher than saline groups ($p < 0.05$, Figure 3D). There was similar tendency for IL-6 ($p < 0.05$, Figure 3E). A small but not significant increase of MIP-2 concentrations in the Fe-poor SWCNT group and a significant increase in the Fe-rich SWCNT group were observed at 72 h post-exposure ($p < 0.05$, Figure 3F). The present data indicate a rapid response of pro-inflammatory mediators (MIP-2, IL-6, and TNF- α) to SWCNT exposure. MIP-2 plays a key role in inflammatory cell recruitment since MIP-2 levels have often preceded the increases in PMN. In addition to pro-inflammatory cytokines, anti-inflammatory cytokine (CC16) were also examined. CC16, the lung damage marker in BALF, was increased significantly after exposure to Fe-poor and Fe-rich CNTs compared to their controls at 24 h post-exposure ($p < 0.01$, Figure 3G). However, compared with the data at 24 h post-exposure a sharp decrease of CC16 values was observed at 72 h post-exposure but still significantly higher than control animals (7-fold and 8.3-fold, respectively, $p < 0.01$, Figure 3G). As a sensitive marker for oxidative stress, the HO-1 values in

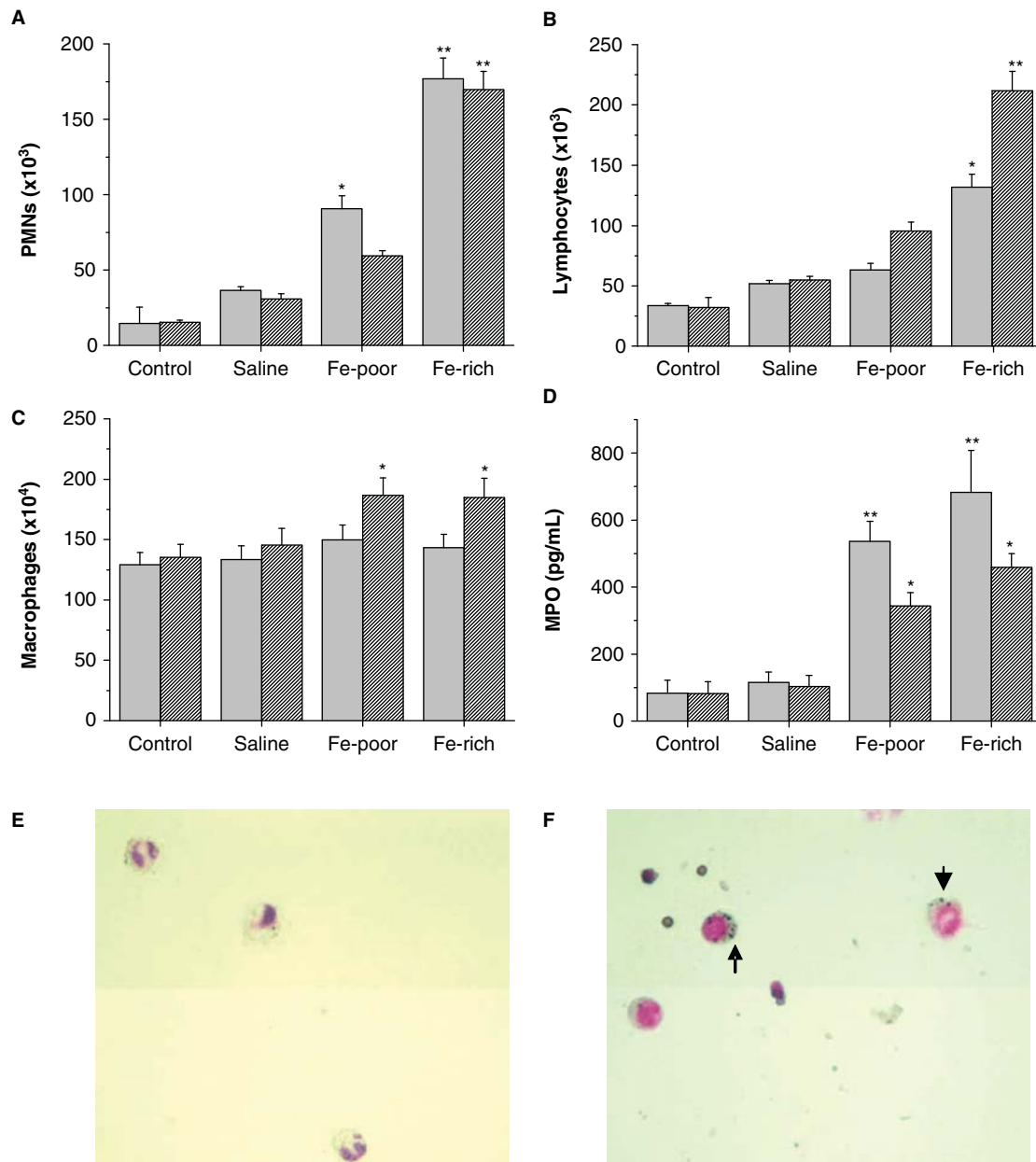


Figure 2. Inflammation marker. (A) PMN number (B) lymphocyte number (C) macrophage number (D) MPO content (E) neutrophil cells (20×) (F) SWCNTs (arrow)-laden macrophage cells (20×) in BALF measured at 24 and 72 hours after exposure. SH rats were exposed to saline or SWCNTs by intratracheal instillation. Values are expressed as means \pm SD and $n = 6$. * $p < 0.05$ vs. saline group at same time point; ** $p < 0.01$ vs. saline group at same time point.

BALF were significantly increased at 24 h post-exposure ($p < 0.05$) and significantly decreased ($p < 0.05$) to the normal level at 72 h post-exposure (Figure 3H). Higher levels of CC16 and HO-1 were induced by exposure to Fe-rich CNT than Fe-poor CNT (no significance).

Additionally, an upper induction of Endothelin-1 (ET-1) in BALF was observed at 24 h post-exposure suggesting that CNT exposure induced endothelial

dysfunction in the pulmonary circulation ($p < 0.05$, Figure 3I).

Blood analysis

We found a significant increase in white blood cells and lymphocytes and no significant changes in other hematological parameters in SWCNT-exposed SH rats (data not shown). The serum was

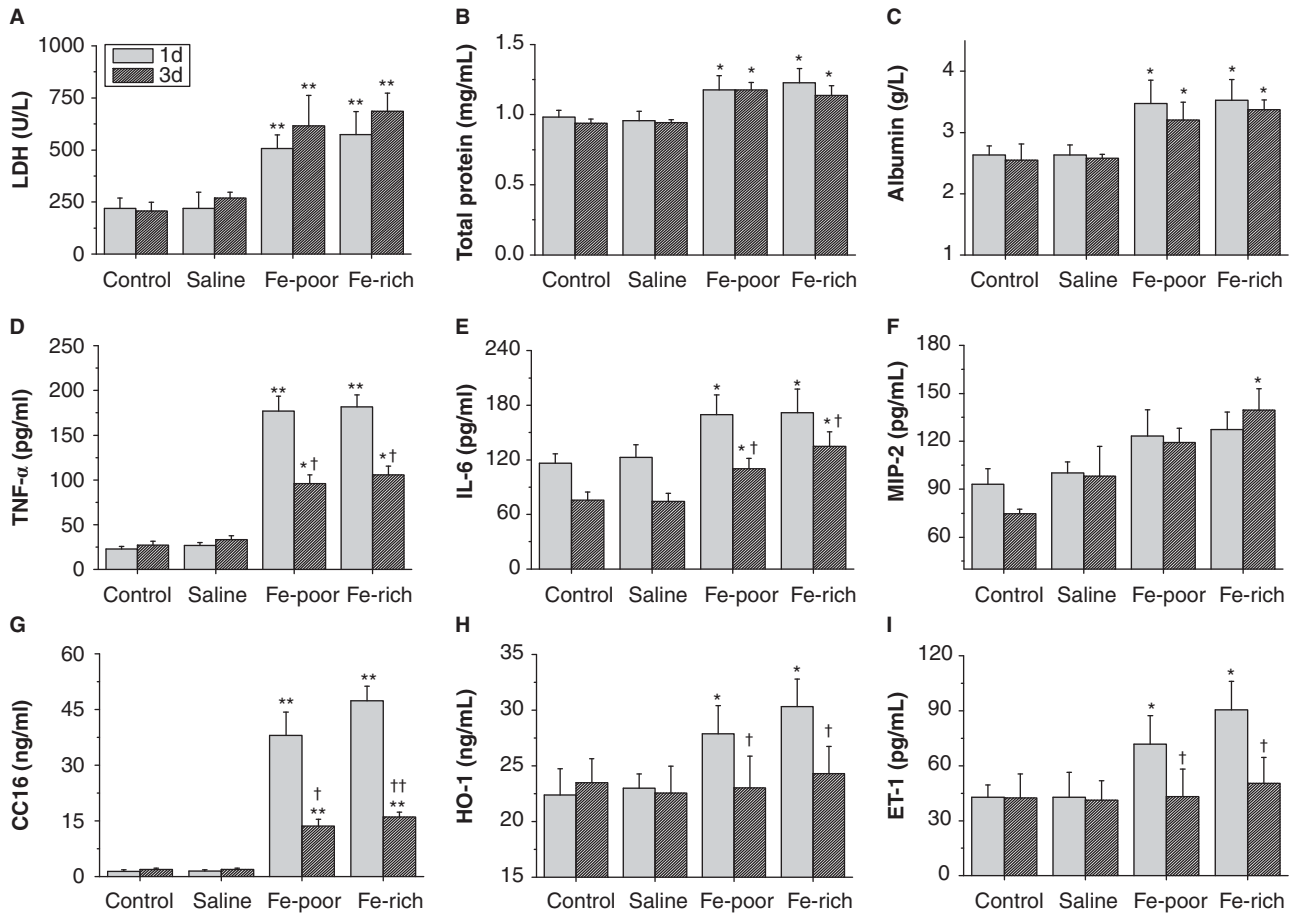


Figure 3. Toxicity markers, cytokines and ET-1 content in BALF measured at 24 and 72 hours after exposure. (A) LDH activity, (B) total protein, (C) albumin, (D) TNF- α , (E) IL-6, (F) MIP-2, (G) CC16, (H) HO-1 and (I) ET-1 contents in BALF measured at 24 and 72 hours after exposure. * $p < 0.05$ vs. saline group at same time point, ** $p < 0.01$ vs. saline group at same time point; † $p < 0.05$ vs. 24 hours post-exposure at same SWCNTs, †† $p < 0.01$ vs. 24 hours post-exposure at same SWCNTs.

also harvested to evaluate the hepatic function with levels of alanine aminotransferase (ALT, EC 2.6.1.2) and aspartate aminotransferase (AST, EC 2.6.1.1), renal function with levels of creatinine (Cr), myocardial lesion with levels of creatine kinase (CK, EC 2.7.3.2) and LDH using a Biochemical Autoanalyzer (Type 7170, Hitachi, Japan). AST/ALT was also determined, which can sometimes help determine whether the liver or another organ has been damaged. Compared with control, a significant increase of ALT was found in Fe-rich SWCNT at 72 h post-exposure ($p < 0.05$, Figure 4A). AST, AST/ALT, CK, LDH were significantly increased at 24 h post-exposure comparing to saline group, which indicated that SWCNTs exposure caused acute liver damage and cardiac damage ($p < 0.05$, Figures 4B, 4C, 4D, 4E). These lesions can be recovered to a great extent because all four biomarkers were significantly decreased at 72 h post-exposure ($p < 0.05$). In addition, no significant change was observed for Cr (Figure 4F).

Cardiovascular effects

Among blood parameters related to coagulation and vasoconstriction, a significant increase of fibrinogen in the plasma was only found in Fe-rich CNT-treated animals ($p < 0.05$, Figure 5A). Significant increases of ET-1 and ACE in the plasma were found both CNT-treated groups ($p < 0.05$, Figure 5B and 5C). Endothelin-1 is the most potent vasoconstrictive substance known and has a key role in vascular homeostasis. Its over-expression would contribute to high blood pressure (hypertension) and heart disease. Angiotensin-converting enzyme regulates blood pressure and is an important target in the management of hypertension. It has two primary functions: ACE catalyses the conversion of angiotensin I to angiotensin II, a potent vasoconstrictor in a substrate concentration dependent manner and ACE degrades bradykinin, a potent vasodilator, and other vasoactive peptides. Under normal conditions, angiotensin II plays a positive role in maintaining blood pressure,

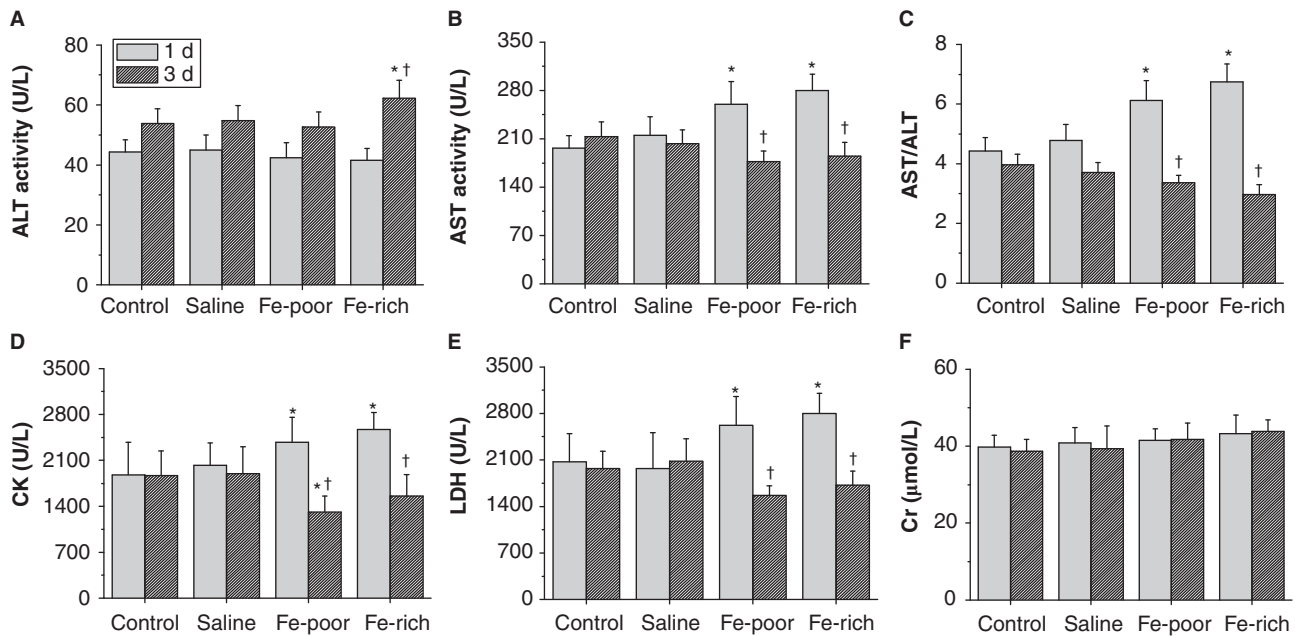


Figure 4. Serum biochemistry. (A) ALT activity, (B) AST activity, (C) AST/ALT, (D) CK activity, (E) LDH activity, and (F) Cr contents in serum measured at 24 and 72 hours after exposure. * $p < 0.05$ vs. saline group at same time point, † $p < 0.05$ vs. 24 hours post-exposure at same SWCNTs.

but in pathological cases, the over-production of angiotensin II would raise blood pressure and result in damage of heart, brain and kidney. However, no significant changes of vWF in plasma and TNF- α , CRP, ICAM-1 in serum were observed within 72 h post exposure (Figures 5D–G).

Histopathology

Lung. Morphological alterations in lungs from SH rats were evaluated by HE staining as shown in Figure 6. Compared with control and saline group (Figure 6A and 6B) the major histopathological lesions after instilled SWCNTs were pulmonary inflammation and multifocal granuloma formation. The most noticeable thing was that considerable amounts of SWCNTs were aggregated in alveoli and formed granuloma along with amounts of inflammatory cells after 24 h exposure (Figure 6C, 6D). This was highly unusual and the hypersensitive granulomatous response represented an attempt to sequester the instilled carbon nanotubes in alveolar cavity. The inflammatory cells including PMNs, macrophages and lymphocytes were found to infiltrate into the pulmonary alveoli (Figure 6E, insert) and these phenomena gradually enhanced at 72 h (Figure 6E, 6F). Generally, the lung lesion of Fe-rich SWCNTs group was much severer and more diffusive than that of Fe-poor SWCNTs group. In addition to alveoli injury, bronchioalveolar epithelia were not kept intact and some dropped epithelial cells fell to tissue

cavity leading to basement membrane damage (Figure 6D). It was interesting to note that vessel wall of pulmonary arteriole became of stenosis that was likely due to the increasing higher blood pressure following pulmonary inflammation (Figure 6F).

Heart. SWCNTs exposure resulted in histological lesions in left ventricle of SH rats. These lesions were characterized by increasing disordered reconstruction of arterial vessel and perivascular myocytes degeneration (Figure 7). The control and saline group presented mild disordered arrangement of blood vessel cell in arteriole (Figure 7A, 7B). In the SWCNTs exposure groups, we found thickened arterial vessel, edema and even leakage of red blood cell (Figure 7C, 7D). The results showed that myofiber degeneration was more commonly observed in hearts from rats exposed to SWCNTs group. Small clusters of perivascular myocytes that were shrunken and rounded hyper eosinophilia occurred (Figure 7C). Lossen ordered myocardial fibre and ruptured fibre were also observed (Figure 7C, 7D). The heart damage was more pronounced at 72 h than following 24 h exposure and also more remarkable in Fe-rich SWCNTs than Fe-poor SWCNTs group.

TEM inspection

Lung. TEM inspection results showed normal ultrastructure of alveolar epithelium of type I cell and alveolar-capillary barrier in the control group

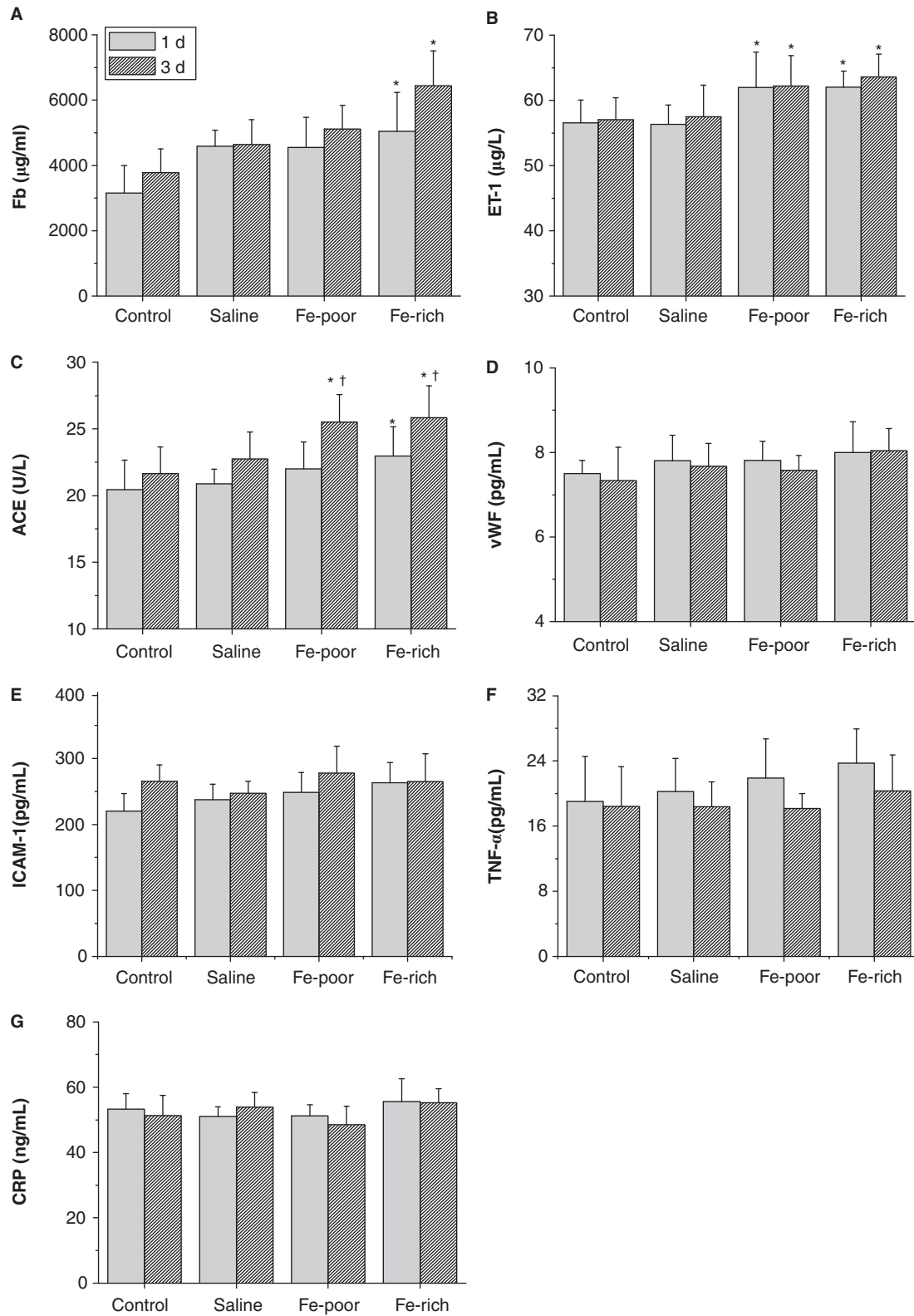


Figure 5. Blood biochemical parameters related to coagulation and vasodilatation. (A) Fb, (B) ET-1, (C) ACE, (D) vWF in plasma, (E) ICAM-1, (F) TNF- α and (G) CRP in serum measured at 24 and 72 hours after exposure. * $p < 0.05$ vs. saline group at same time point, † $p < 0.05$ vs. 24 hours post-exposure at same SWCNTs.

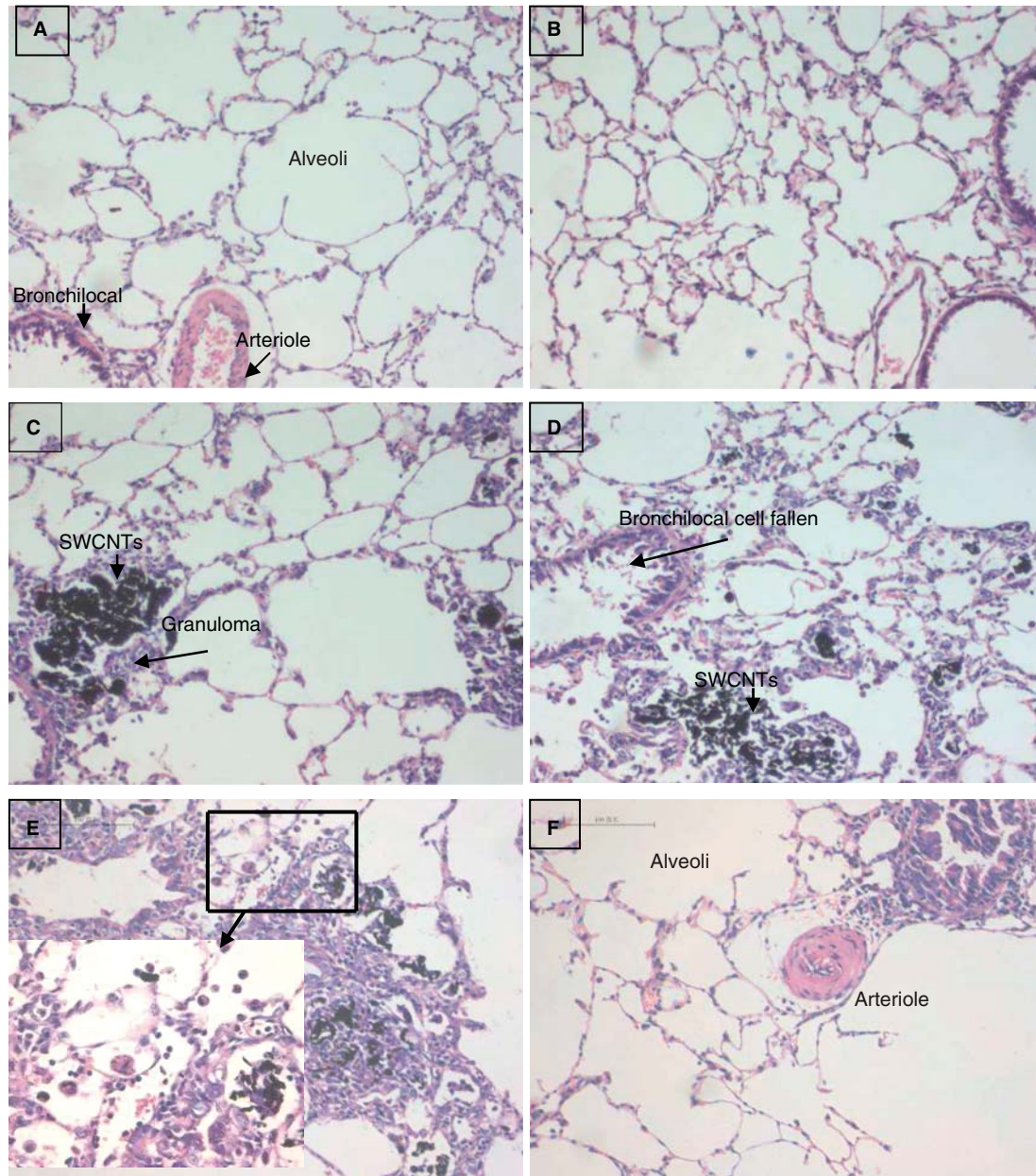


Figure 6. Light micrographs of lung tissue from SH rats exposed to SWCNTs. (A) Control; (B) Saline; (C–D) Fe-poor and Fe-rich SWCNTs groups at 24 h post-exposure, respectively; (E) Fe-rich SWCNTs groups at 72 h post-exposure. Inset: higher magnifications show numerous inflammatory cells infiltration; (F) Fe-poor SWCNTs groups at 72 h post-exposure. Large arrows indicate multifocal granuloma; small arrows, SWCNTs. Bars = 100 μ m for A–D.

(Figure 8A). After SWCNT exposure, we found partial rupture of the basement membrane of type I cell, evacuation of lamellar body and vacuolated mitochondria of type II cell (Figure 8B). PMN in blood cavity of capillary and karyopyknosis of epithelial cells also appeared (Figure 8C). Along with swallowing SWCNTs, vacuolated mitochondria, secondary lysosomes were observed in macrophage (Figure 8D). Cluster of black SWCNTs were located

in the large pinocytotic vesicles of macrophage and the basement of alveolar epithelium cell (Figure 8C, 8D). The above results suggest that acute pathological changes in lung tissues upon SWCNTs exposure are in agreement with the result of increasing total inflammatory cell numbers in BALF.

Heart. Ultrastructural observation showed basically normal nucleus, mitochondria, smooth endoplasmic

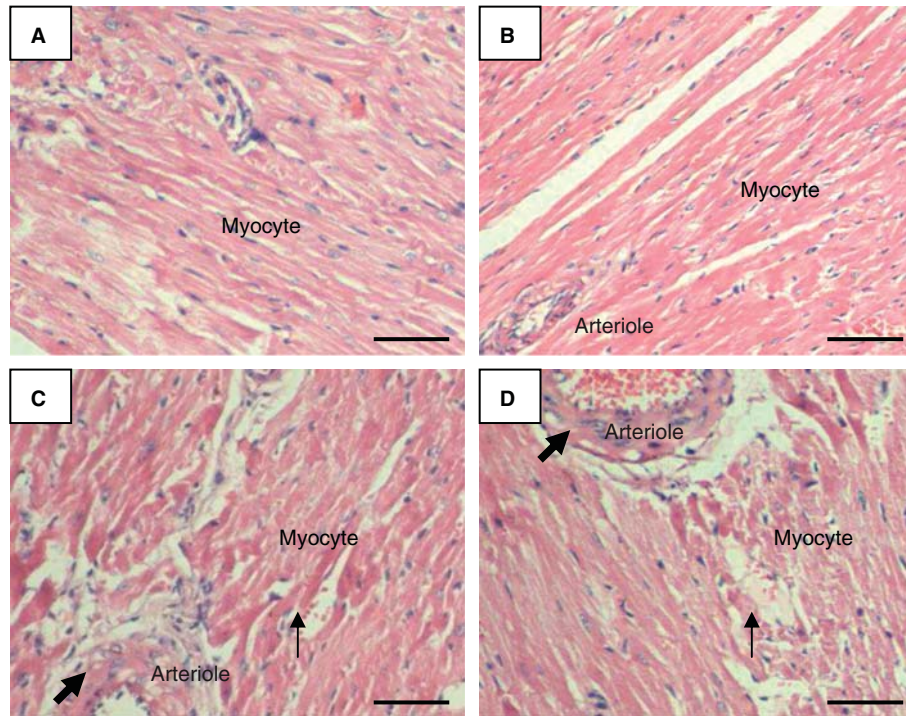


Figure 7. Light micrographs of heart tissue from SH rats exposed to SWCNTs after 24 h. (A) Control; (B) saline; (C) Fe-rich SWCNTs groups; (D) Fe-poor SWCNTs groups. Large arrows indicate disordered arrangement arteriole; small arrows, shrunken or ruptured myocytes. Bars = 100 μ m for A–D.

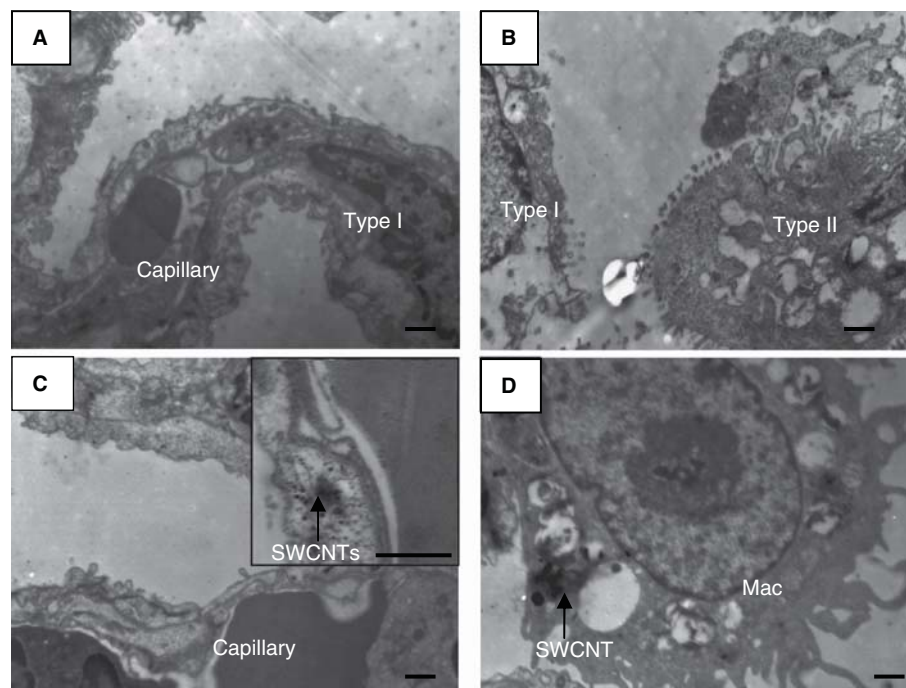


Figure 8. Ultrastructure observation of lung tissue from SH rats exposed to SWCNTs. (A) Control; (B) Fe-poor SWCNTs groups after 24 h; (C, D) Fe-rich SWCNTs groups after 24 h, inset: CNT in the basement of alveolar epithelium cell. Abbreviations: Mac, macrophage; Type I, type I alveolar epithelium cell; Type II, type II alveolar epithelium cell. Arrows indicate SWCNTs. Bars = 500 nm for A–D.

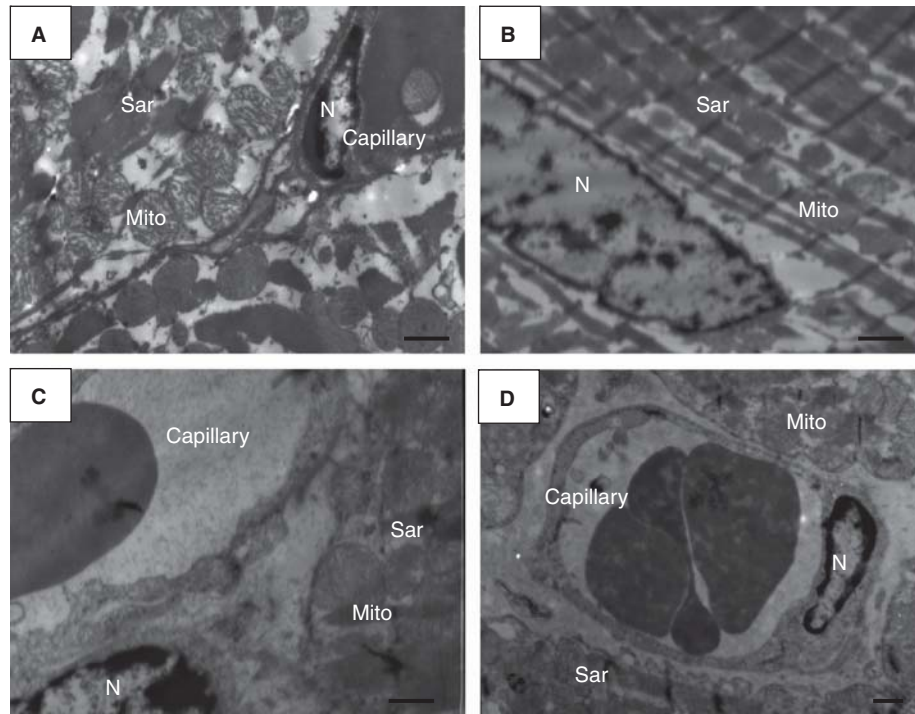


Figure 9. Ultrastructure observation of heart tissue from SH rats exposed to SWCNTs after 24 h. (A) Control; (B) saline; (C) Fe-rich SWCNTs groups; (D) Fe-poor SWCNTs groups. Abbreviations: Sar, sarcomere; Mito, mitochondria; N, nuclear. Bars = 500 nm for A–D.

reticulum (ER) (Figure 9A), and Z line, A band, I band, H band and M line in the sarcomere of the control and saline group (Figure 9B). In the group of exposure to SWCNTs, we observed the presence of capillary congestion and a spongy appearance with tissue rarefaction and vacuolization of epithelial cell, indicating the presence of vasogenic edema and loosened stroma with additional thrombosis and diapedesis of blood (Figure 9C, 9D). The electron microscopy also demonstrated swelling mitochondria, expanded ER and marginated chromatin in myocytes (Figure 9C) and compressed or shrunken cardiac fibre originating from agglomerated Z line of partial cardiac muscle fibre (Figure 9D).

Discussion

The present study demonstrates that exposure to SWCNTs can cause adverse effects on pulmonary and cardiovascular system in a susceptible animal model of high blood pressure. Exposure to CNTs by intratracheal instillation can cause acute and strong lung injury including inflammatory, oxidative stress and toxicity, which can be drawn from the data of cell counts, MPO, LDH, albumin, protein, TNF- α , IL-6, MIP-2, CC16 and HO-1. SWCNTs with high contents of metal impurities induced much greater

adverse responses. The major lung histopathological lesions after instilling SWCNTs were pulmonary inflammation, multifocal granuloma formation and a diffuse pattern of carbon nanotube particulate deposition in alveoli as well as broncholoc cell hypotrophy or fallen (Figure 6). The changes of AST, ALT, AST/ALT, LDH, and CK in the serum suggest pulmonary exposure to CNTs can also cause acute systemic damages including liver damage and myocardial damage. Increased endothelin-1 in BALF and plasma, and angiotensin I-converting enzyme in plasma, indicated endothelial dysfunction in the pulmonary circulation and peripheral vascular thrombosis.

Uptake of SWCNTs in the lungs activates inflammation via two likely ways. The first way consists of generation of pro-inflammatory cytokines by macrophages that have phagocytized SWCNTs. The mediators released by alveolar macrophages (AMs) following phagocytosis can trigger local and systemic inflammatory responses. The second way includes the induction of chemokine produced by pulmonary epithelium. After phagocytizing inhaled SWCNTs, lung epithelial cells can synthesize series of pro-inflammatory mediators including cytokines and chemokines, which influence local and systemic inflammation. Following SWCNTs inhalation, release of these mediators by alveolar macrophage further accelerates the

release of PMN cells and monocytes from the bone marrow, thus inflammation is elicited. Finally, cytokines can stimulate liver to release proteins which involve in the acute phase of the systemic inflammatory response.

The process of inflammation includes inflammatory and anti-inflammatory responses that usually maintain homeostasis. Therefore, we further examined HO-1 and CC16 related to anti-inflammation. The extremely increased levels of CC16 and HO-1 at 24 h and quick reduction at 72 h post-exposure (Figure 3G, 3H) agreed that in underlying cardiac disease animals, host compensatory responses to injury or increased oxidative burden usually led to increase in tissue anti-oxidant levels. The transient and tremendous increase of CC16 indicated the exposure produce an acute and retrievable inflammatory response. Clara cell protein is regarded as one of the major secretory proteins protecting the respiratory tract against oxidative stress, inflammation and fibrosis in lung (Mantile et al. 1993). The induced HO-1 expression was an indicator of a host defense mechanism for oxidative stress and was likely to be directly activated by SWCNTs, which had been shown to provide a substantial oxidative potency. The pathological changes of cardiac tissues demonstrated that SWCNTs exposure resulted in increases of histological lesions in SH rats by increasing disordered reconstruction of arterial vessel and perivascular myocytes degeneration and could be considered as an acute reaction of the vascular endothelium. On the basis of these findings, we conclude that a close relationship exists between SWCNTs exposure and increased cardiovascular risk including impairment in endothelial function and vascular activity.

Recent publications on the biodistribution and translocation of CNTs have shown they may move from lung tissues to the circulation. The ^{14}C -labelled MWCNTs in the lung were gradually eliminated from 78% at 1 day post-exposure to 20% at 28 days post-instillation (Deng et al. 2007). The secretion of the respiration tract following endocytosis of macrophages and/or subsequent cilia escalator may help the removal from lung tissues. Additionally, the over-loaded MWCNTs may flow to the afferent lymphatics, and even the capillaries. We observed the pulmonary inflammation and granuloma formation whereas the lung was laden with SWCNTs (Figure 6C, 6D). Indeed, aggregated SWCNT particles are not efficiently cleared via mucociliary or macrophage-mediated mechanisms and are, thus, likely to be taken up by epithelial cells and translocated to extrapulmonary sites. *In vitro* study showed that carbon nanotubes damaged the endothelial cells

with a resultant increase in permeability (Walker et al. 2009). However, this hypothesis still needs to be strengthened since there is still a notable uncertainty about the significant translocation of inhaled SWCNTs *in vivo* (Lam et al. 2004; Warheit et al. 2004; Deng et al. 2007; Shvedova et al. 2008).

The present results show that the increased fibrinogen level 3 days later might increase the risk of peripheral vascular thrombosis since fibrinogen is a risk factor for cardiovascular disease and a pro-coagulant product of the endothelium. Endothelin-1 is the most potent vasoconstrictive substance known and has a key role in vascular homeostasis. Significant increases of ET-1 and ACE in plasma were found in both CNT-treated groups. Its over-expression would contribute to high blood pressure (hypertension) and heart disease. Angiotensin-converting enzyme regulates blood pressure and is an important target in the management of hypertension. It has two primary functions: ACE catalyses the conversion of angiotensin I to angiotensin II, a potent vasoconstrictor in a substrate concentration dependent manner and ACE degrades bradykinin, a potent vasodilator, and other vasoactive peptides. Under normal conditions angiotensin II plays a positive role in maintaining blood pressure, but in pathological cases, the over-production of angiotensin II will raise blood pressure and result in damage of heart, brain and kidney. However, the changes of plasma CRP, vWF, TNF- α and ICAM-1 were not observed. The previous studies showed UFP exposure can induce changes in numerous proteins associated with coagulation, including CRP, plasminogen activator inhibitor-1, fibrinogen, and vWF. Endothelial lesions, in fact, triggered intense proliferate signals which had an effect on smooth muscle cells, and then exacerbated the cardiac injury (Pope et al. 2004; Shvedova et al. 2005). It is however still possible that the unique nature of the SWCNTs caused the release of specific vasoactive mediators that were responsible for later cardiovascular dysfunction for a long-term exposure.

Many unique physiochemical parameters including surface functional groups, surface chemistry, tube dimensions, and metal catalyst residues can greatly influence the biological effects of CNTs (Sayes et al. 2006; Kostarelos 2008; Walker et al. 2009; Wang et al. 2009), which somehow brought conflicting data when revisiting the previous reports. Commercially available SWCNTs are highly diverse materials whose character and constituents vary with the production scheme and post-fabrication treatment (Plata et al. 2008). Since the diversity of metal catalysts used in nanotube synthesis, there is no universal

metal 'fingerprint' for all SWCNTs. It is impossible to completely remove metal residues, although many purification methods are developed on the premise of preserving the structure of CNT (Mohanapriya and Lakshminarayanan 2007; Pumera 2007). Our previous studies have shown the existence of significant quantity of metal residues in commercial CNTs and indicated arranging from 0.44–3 wt.% of catalyst residues remained even suffering strong and careful purification processes (Ge et al. 2008; Plata et al. 2008).

Currently, there are different opinions about the role of metal residues playing in the toxicological effects caused by CNTs. Some reports suggested that CNT itself instead of metal catalyst causes toxicological effects to biological system (Cheng et al. 2009). They found that cells treated with purified MWCNTs and the main contaminant Fe_2O_3 itself yielded toxicity only from the nanotubes and not from the Fe_2O_3 . The other reports indicated that both CNT itself and metal catalytic residues would attribute to the toxicological effects (Kagan et al. 2006; Murray et al. 2009). Our study demonstrated that the existence of metal residues in CNTs can aggravate the adverse effects induced by CNTs. It is known that transitional metal can take part in Fenton reaction and produce free radical that can induce cell damage through protein oxidation, lipid oxidation, DNA strand breaks, and covalent modification of DNA (Wolff 1993; Ercal et al. 2001; Valko et al. 2006). Therefore during the investigation of the biological effects of CNT, metal residues should be taken into consideration. The metals are fully encapsulated based on TEM observation in CNT synthesis and manufacturing as well as the common observation that oxidation is required to damage the carbon shells before significant quantities of metal can be removed by strong acid treatment. Our data show that iron mobilization into artificial lysosomal fluid is quite high and 33.4% of total in SWCNT can be mobilized. We hypothesize that enhanced uptake of Fe or other metals is due to acid lysosomal microenvironment that make more catalytic residues in SWCNTs dissolved once uptaken by cells *in vivo*. The enhanced adverse effects of Fe-rich SWCNTs should have a close relationship to the uptake and bioavailability of Fe or other metals, in which the small amounts are accessible and sufficient to produce toxicological significance.

Conclusion

In conclusion, our findings illustrate that exposure to SWCNTs by two intratracheal instillations in SH rats can induce local inflammatory response and oxidative

stress in lung tissues as well as the reconstruction of arterial vessel, perivascular myocytes degeneration and peripheral vascular lesions. These results indicate that SWCNTs exposure in SH rats can induce lesion of cardiovascular system and suggest that individuals with existing cardiovascular diseases are very susceptible to SWCNT stimuli. The present study also highlights the importance of metal impurities in CNTs contributed to cardiovascular injury that exposure to CNTs with higher metal contents brings more pronouncedly adverse responses. However, the underlying patho-physiological mechanisms or factors linking SWCNTs and cardiovascular morbidity need further investigation.

Declaration of interest: We acknowledge the financial support from the Ministry of Science and Technology of China (Nos. 2011CB933401, 2009AA3Z335 and 2010CB934004), National Natural Science Foundation of China (10975040) and the CAS Knowledge Innovation Program. The authors report no conflicts of interest. The authors alone are responsible for the content and writing of the paper.

References

- Badr K, Wainwright CL. 2004. Inflammation in the cardiovascular system: Here, there and everywhere. *Curr Opin Pharmacol* 4(2):107.
- Bagate K, Meiring JJ, Gerlofs-Nijland ME, Vincent R, Cassee FR, Borm PJA. 2004. Vascular effects of ambient particulate matter instillation in spontaneous hypertensive rats. *Toxicol Appl Pharmacol* 197(1):29–39.
- Cao Q, Zhang S, Dong C, Song W. 2007. Pulmonary responses to fine particles: Differences between the spontaneously hypertensive rats and wistar kyoto rats. *Toxicol Lett* 171(3): 126–137.
- Cheng C, Müller KH, Koziol KKK, Skepper JN, Midgley PA, Welland ME, et al. 2009. Toxicity and imaging of multi-walled carbon nanotubes in human macrophage cells. *Biomaterials* 30(25):4152–4160.
- Chou CC, Hsiao HY, Hong QS, Chen CH, Peng YW, Chen HW, et al. 2008. Single-walled carbon nanotubes can induce pulmonary injury in mouse model. *Nano Lett* 8(2):437–445.
- Delfino RJ, Staimer N, Tjoa T, Polidori A, Arhami M, Gillen DL, et al. 2008. Circulating biomarkers of inflammation, antioxidant activity, and platelet activation are associated with primary combustion aerosols in subjects with coronary artery disease. *Environ Health Perspect* 116(7):898.
- Deng X, Jia G, Wang H, Sun H, Wang X, Yang S, et al. 2007. Translocation and fate of multi-walled carbon nanotubes in vivo. *Carbon* 45(7):1419–1424.
- Donaldson K, Stone V, Seaton A, MacNee W. 2001. Ambient particle inhalation and the cardiovascular system: Potential mechanisms. *Environ Health Perspect* 109:523–527.
- Elder A, Couderc JP, Gelein R, Eberly S, Cox C, Xia X, et al. 2007. Effects of on-road highway aerosol exposures on autonomic responses in aged, spontaneously hypertensive rats. *Inhal Toxicol* 19(1):1–12.

- Ercal N, Gurer-Orhan H, Aykin-Burns N. 2001. Toxic metals and oxidative stress. Part I: Mechanisms involved in metal-induced oxidative damage. *Curr Top Med Chem* 1(6): 529–539.
- Erdely A, Hulderman T, Salmen R, Liston A, Zeidler-Erdely PC, Schwegler-Berry D, et al. 2008. Cross-talk between lung and systemic circulation during carbon nanotube respiratory exposure. Potential biomarkers. *Nano Lett* 9(1):36–43.
- Gauderman WJ, Avol E, Gilliland F, Vora H, Thomas D, Berhane K, et al. 2004. The effect of air pollution on lung development from 10 to 18 years of age. *New Engl J Med* 351(11):1057–1067.
- Ge C, Lao F, Li W, Li Y, Chen C, Qiu Y, et al. 2008. Quantitative analysis of metal impurities in carbon nanotubes: Efficacy of different pretreatment protocols for ICPMS spectroscopy. *Anal Chem* 80(24):9426–9434.
- Guo L, Morris DG, Liu X, Vaslet C, Hurt RH, Kane AB. 2007. Iron bioavailability and redox activity in diverse carbon nanotube samples. *Chem Mater* 19(14):3472–3478.
- Kagan VE, Tyurina YY, Tyurin VA, Konduru NV, Potapovich AI, Osipov AN, et al. 2006. Direct and indirect effects of single walled carbon nanotubes on RAW 264.7 macrophages: Role of iron. *Toxicol Lett* 165(1):88–100.
- Kobayashi N, Naya M, Ema M, Endoh S, Maru J, Mizuno K, et al. 2010. Biological response and morphological assessment of individually dispersed multi-wall carbon nanotubes in the lung after intratracheal instillation in rats. *Toxicol* 276(3):143–153.
- Kostarelos K. 2008. The long and short of carbon nanotube toxicity. *Nat Biotechnol* 26(7):774–776.
- Lam CW, James JT, McCluskey R, Hunter RL. 2004. Pulmonary toxicity of single-wall carbon nanotubes in mice 7 and 90 days after intratracheal instillation. *Toxicol Sci* 77(1):126.
- Li Z, Hulderman T, Salmen R, Chapman R, Leonard SS, Young SH, et al. 2007. Cardiovascular effects of pulmonary exposure to single-wall carbon nanotubes. *Environ Health Perspect* 115(3):377.
- Liu LJS, Box M, Kalman D, Kaufman J, Koenig J, Larson T, et al. 2003. Exposure assessment of particulate matter for susceptible populations in Seattle. *Environ Health Perspect* 111(7):909.
- Liu X, Guo L, Morris D, Kane AB, Hurt RH. 2008. Targeted removal of bioavailable metal as a detoxification strategy for carbon nanotubes. *Carbon* 46(3):489–500.
- Liu X, Gurel V, Morris D, Murray DW, Zhitkovich A, Kane AB, et al. 2007. Bioavailability of nickel in single-wall carbon nanotubes. *Adv Mater* 19(19):2790–2796.
- Ma-Hock L, Treumann S, Strauss V, Brill S, Luizi F, Mertler M, et al. 2009. Inhalation toxicity of multi-wall carbon nanotubes in rats exposed for 3 months. *Toxicol Sci* 112(2): 468–481.
- Mantile G, Miele L, Cordella-Miele E, Singh G, Katyal SL, Mukherjee AB. 1993. Human Clara cell 10-kDa protein is the counterpart of rabbit uteroglobin. *J Biol Chem* 268(27):20343.
- Mitchell LA, Gao J, Wal RV, Gigliotti A, Burchiel SW, McDonald JD. 2007. Pulmonary and systemic immune response to inhaled multiwalled carbon nanotubes. *Toxicol Sci* 100(1): 203.
- Mohanapriya S, Lakshminarayanan V. 2007. Simultaneous purification and spectrophotometric determination of nickel present in as-prepared single-walled carbon nanotubes (SWCNT). *Talanta* 71(1):493–497.
- Muller J, Huaux F, Fonseca A, Nagy JB, Moreau N, Delos M, et al. 2008. Structural defects play a major role in the acute lung toxicity of multiwall carbon nanotubes: Toxicological aspects. *Chem Res Toxicol* 21(9):1698–1705.
- Muller J, Huaux F, Moreau N, Misson P, Heilier JF, Delos M, et al. 2005. Respiratory toxicity of multi-wall carbon nanotubes. *Toxicol Appl Pharmacol* 207(3):221–231.
- Murray AR, Kisin E, Leonard SS, Young SH, Kommineni C, Kagan VE, et al. 2009. Oxidative stress and inflammatory response in dermal toxicity of single-walled carbon nanotubes. *Toxicology* 257(3):161–171.
- Plata DL, Gschwend PM, Reddy CM. 2008. Industrially synthesized single-walled carbon nanotubes: Compositional data for users, environmental risk assessments, and source apportionment. *Nanotechnology* 19:185706.
- Pope CA III, Burnett RT, Thurston GD, Thun MJ, Calle EE, Krewski D, et al. 2004. Cardiovascular mortality and long-term exposure to particulate air pollution. *Circulation* 109(1):71–77.
- Poland CA, Duffin R, Kinloch I, Maynard A, Wallace WAH, Seaton A, et al. 2008. Carbon nanotubes introduced into the abdominal cavity of mice show asbestos-like pathogenicity in a pilot study. *Nature Nanotech* 3(7):423–428.
- Porter DW, Hubbs AF, Mercer RR, Wu N, Wolfarth MG, Sriram K, et al. 2010. Mouse pulmonary dose-and time course-responses induced by exposure to multi-walled carbon nanotubes. *Toxicology* 269(2–3):136–147.
- Pulskamp K, Diabaté S, Krug HF. 2007. Carbon nanotubes show no sign of acute toxicity but induce intracellular reactive oxygen species in dependence on contaminants. *Toxicol Lett* 168(1): 58–74.
- Pumera M. 2007. Carbon nanotubes contain residual metal catalyst nanoparticles even after washing with nitric acid at elevated temperature because these metal nanoparticles are sheathed by several graphene sheets. *Langmuir* 23(11): 6453–6458.
- Rückerl R, Phipps RP, Schneider A, Frampton M, Cyrus J, Oberdörster G, et al. 2007. Ultrafine particles and platelet activation in patients with coronary heart disease – results from a prospective panel study. Part I. *Fibre Toxicol* 4(1): 1743–8977.
- Ryman-Rasmussen JP, Cesta MF, Brody AR, Shipley-Phillips JK, Everitt JJ, Tewksbury EW, et al. 2009. Inhaled carbon nanotubes reach the subpleural tissue in mice. *Nature Nanotech* 4(11): 747–751.
- Samet JM, Dominici F, Currier FC, Coursac I, Zeger SL. 2000. Fine particulate air pollution and mortality in 20 US cities, 1987–1994. *New Engl J Med* 343(24):1742.
- Sayes CM, Liang F, Hudson JL, Mendez J, Guo W, Beach JM, et al. 2006. Functionalization density dependence of single-walled carbon nanotubes cytotoxicity in vitro. *Toxicol Lett* 161(2):135–142.
- Shvedova AA, Kisin E, Murray AR, Johnson VJ, Gorelik O, Arepalli S, et al. 2008. Inhalation vs. aspiration of single-walled carbon nanotubes in C57BL/6 mice: Inflammation, fibrosis, oxidative stress, and mutagenesis. *Am J P- Lung* 295(4): L552.
- Shvedova AA, Kisin ER, Mercer R, Murray AR, Johnson VJ, Potapovich AI, et al. 2005. Unusual inflammatory and fibrogenic pulmonary responses to single-walled carbon nanotubes in mice. *Am J P- Lung* 289(5):L698.
- Smart SK, Cassady AI, Lu GQ, Martin DJ. 2006. The biocompatibility of carbon nanotubes. *Carbon* 44(6):1034–1047.
- Valko M, Rhodes CJ, Moncol J, Izakovic M, Mazur M. 2006. Free radicals, metals and antioxidants in oxidative stress-induced cancer. *Chem Biol Interact* 160(1):1–40.
- Vanhoutte PM. 1997. Endothelial dysfunction and atherosclerosis. *Eur Heart J* 18(Suppl. E):19.

- Walker VG, Li Z, Hulderman T, Schwegler-Berry D, Kashon ML, Simeonova PP. 2009. Potential in vitro effects of carbon nanotubes on human aortic endothelial cells. *Toxicol Appl Pharmacol* 236(3):319–328.
- Wang X, Jia G, Wang H, Nie H, Yan L, Deng XY, et al. 2009. Diameter effects on cytotoxicity of multi-walled carbon nanotubes. *J Nanosci Nanotech* 9(5):3025–3033.
- Warheit DB, Laurence BR, Reed KL, Roach DH, Reynolds GAM, Webb TR. 2004. Comparative pulmonary toxicity assessment of single-wall carbon nanotubes in rats. *Toxicol Sci* 77(1):117.
- Wolff SP. 1993. Diabetes mellitus and free radicals: Free radicals, transition metals and oxidative stress in the aetiology of diabetes mellitus and complications. *Br Med Bull* 49(3):642.

Supplementary material available online

Supplementary Tables S1 and S2.